

# Nuclear Shadowing in the Holographic Framework

L. Agozzino<sup>a,b</sup>, P. Castorina<sup>a,b</sup>, and P. Colangelo<sup>c</sup>

<sup>a</sup>*Dipartimento di Fisica, Università di Catania, via S. Sofia 62, 95125 Catania, Italy*

<sup>b</sup>*INFN, Sezione di Catania, via S. Sofia 62, 95125 Catania, Italy*

<sup>c</sup>*INFN, Sezione di Bari, via Orabona 4, 70126 Bari, Italy*

The nucleon structure function  $F_2^N$  computed in a holographic framework can be used to describe nuclear deep inelastic scattering effects provided that a rescaling of the  $Q^2$  momentum and of the IR hard-wall parameter  $z_0$  is made. The ratios  $R_A = F_2^A/F_2^N$  can be obtained in terms of a single rescaling parameter  $\lambda_A$  for each nucleus. The resulting ratios agree with experiment in a wide range of the shadowing region.

PACS numbers: 11.25.Tq, 11.10.Kk, 12.38.Lg, 24.85.+p

## INTRODUCTION

The AdS/CFT correspondence [1], an important tool to analyze nonperturbative aspects of gauge theories, has been successfully used to study features of QCD [2]. In its application to deep inelastic scattering (DIS) at strong coupling [3, 4], the nucleon structure function  $F_2^N(x, Q^2)$  at small Bjorken variable  $x$  has been represented as the sum of a conformal term and of a contribution due to quark confinement, crucial to fit the data. The evaluation of these contributions requires the holographic nucleon wave function, which is assumed to be peaked at distances  $O(1/Q')$  close to the infrared boundary  $z_0$ , with  $Q'$  of the order of the nucleon mass.

Nonperturbative, confinement dynamics shows up also in the modification of the structure functions of a nucleon in a nucleus. The proposed theoretical models of these effects are based on the effective change of the mean square distances among quarks and gluons in a nuclear environment with respect to the free nucleon case [6].

Nuclear effects are described comparing the structure functions of the nuclear target per nucleon to the free nucleon ones and, for electroproduction, the ratios  $R_A = F_2^A(x, Q^2)/F_2^D(x, Q^2)$  are considered, with  $F_2^A$  and  $F_2^D$  the structure functions per nucleon in the nucleus  $A$  and in deuterium  $D$  (where the nuclear binding is considered negligible). Nuclear modifications depend on  $x$ :  $x \leq 0.1$  is the shadowing region where  $R_A < 1$ ; for large  $x$  one has the so-called EMC effect; in the range  $0.1 < x < 0.25$  there is the anti-shadowing with  $R_A > 1$ , usually obtained by the energy-momentum sum rule. The understanding of these modifications requires to evaluate the “distortion” of the free nucleon wave function due to nuclear binding. In the small- $x$  region, dominated by Pomeron exchange, the AdS/CFT strong coupling BPST Pomeron kernel [7] is a good framework to study nuclear deep inelastic structure functions, provided one knows the holographic baryon wave function in the nucleus. A simplified approach can be based on the observation that the spatial separation between quarks determines the strength of the quark-Pomeron coupling [8]

and that the effective confinement size is modified in a nucleus.

Following this point of view, we consider an approach to shadowing in an AdS/CFT framework, describing the nuclear binding effects on the nucleon wave function through an effective distance  $1/Q'_A$  and an effective confinement boundary  $z_0^A$ , and studying the scaling properties of the holographic structure function  $F_2$  under the change  $Q' \rightarrow Q'_A$  and  $z_0 \rightarrow z_0^A$ . In this way, nuclear effects are described by rescaling the confinement parameters. The results agree with the experimental data.

## APPROACHES TO NUCLEAR DIS EFFECTS

In models of shadowing and EMC effects, the description of the nuclear modifications is based on the change of the effective mean square distance among quarks and gluons in a nuclear environment with respect to the free nucleon case [6].

In the  $x$ -rescaling model the EMC effect is described by rescaling  $x$  in the free nucleon structure function [9],

$$F_2^A(x, Q^2) = F_2^D(x/\hat{z}, Q^2) , \quad (1)$$

with  $\hat{z} \simeq 1 - \epsilon/M$ ,  $M$  the proton mass and  $\epsilon$  the energy necessary to “ionize” a nucleus and make it emit a nucleon. However, the values of  $\epsilon$  able to fit the large- $x$  data exceed the nuclear binding calculations [6].

The  $Q^2$ -rescaling model of EMC effect is based on the relation [10, 11]

$$F_2^A(x, Q^2) = F_2^D(x, \chi_A Q^2) , \quad (2)$$

indicating that the effective  $Q^2$  for a bound nucleon is different from the free nucleon. This dynamical property is investigated here in the holographic framework. It is related to the modification of the quark confinement size in the nucleus [10, 11]: quarks and gluons are no longer confined to specific nucleons, but spread over distances larger than the free nucleon size. By studying the structure function moments, starting from a  $Q^2$  region where the valence picture is a good approximation, one

can show that in QCD, for large  $Q^2$ , this change of scale is connected to the strong coupling constant  $\alpha_s$ . The  $x$ - and  $Q^2$ -rescaling models, although different in their starting points, can be related [12].

The QCD  $Q^2$  dependence of structure functions can be also applied to shadowing at small  $x$ , including the effect of gluon recombination in nuclei which is neglected in the free nucleon evolution equation [13]. Modifying the linear  $Q^2$  evolution equation one shows that the recombination depletes the gluon distribution at small  $x$ , which reflects into a depletion of sea quark distribution [13]. The  $Q^2$  dependence of parton distributions in nuclei based on linear QCD evolution equations at next-to-leading order is described in ref.[14].

A different nonperturbative approach considers that the small- $x$  behavior of  $F_2$  is controlled by Pomeron exchange [15]. In a nuclear environment the effective coupling of the Pomeron to a quark is suppressed because of the nucleon overlap. Although quarks and gluons are no longer confined to specific nucleons but rather spread on distances larger than the free nucleon size, the average spatial separation between quarks before color neutralization decreases, with the Pomeron coupling directly related with this typical size [8].

Hence, a physical description of EMC and shadowing effects can be based on the effective modification of the dynamical scales in deep inelastic scattering on nuclear target respect to the free nucleon case. This rescaling, and in particular the  $Q^2$  one, is a property of the AdS/CFT approach to deep inelastic scattering, not only in the conformal limit but also if the confinement dynamics is taken into account.

## NUCLEAR STRUCTURE FUNCTIONS IN HOLOGRAPHIC FRAMEWORK

The possibility of an approach to DIS on a proton based on AdS/CFT duality was analyzed in the Polchinski-Strassler first proposal [3]. Here we adopt the method in [4], based on the calculation of the virtual  $\gamma^*p$  total cross section, which allows to express, e.g., the structure function  $F_2$  as the sum of two contributions: a model-independent term for conformal gauge theories and an additional non-conformal term accounting for confinement. This latter (model dependent) contribution is obtained by breaking conformal invariance through a sharp cut-off (“hard-wall”) of the AdS holographic space [16].

One starts from the matrix element of two R-currents in a hadron of momentum  $P$  and charge  $\mathcal{Q}$ ,

$$\begin{aligned} T^{\mu\nu} &\equiv i \int d^4y e^{iq \cdot y} \langle P\mathcal{Q} | T[J^\mu(y)J^\nu(0)] | P\mathcal{Q} \rangle \\ &= F_1(x, Q^2) (\eta^{\mu\nu} - \frac{q^\mu q^\nu}{q^2}) \\ &\quad + \frac{2x}{q^2} F_2(x, Q^2) (P^\mu + \frac{q^\mu}{2x})(P^\nu + \frac{q^\nu}{2x}) \end{aligned} \quad (3)$$

(with  $\mu, \nu$  four-dimensional indices,  $\eta^{\mu\nu}$  Minkowski metric,  $x = Q^2/2P \cdot q$  and  $Q^2 = -q^2$ ) which allows to extract the DIS structure functions for electron-hadron scattering and, in particular,  $F_2(x, Q^2)$ . The AdS/CFT calculation involves the couplings

$$g_s = \frac{g_{YM}^2}{4\pi} = \alpha_{YM} = \frac{\lambda}{4\pi N_C}, \quad R = \alpha'^{\frac{1}{2}} \lambda^{\frac{1}{4}} \quad (4)$$

with  $g_s \ll 1$  and  $\lambda \gg 1$ .  $R$  is the AdS radius. In the following, the coupling  $\rho = 2/\sqrt{\lambda}$  is used.

The dual string calculation of the matrix element (3), or of its imaginary part appearing in DIS processes, describes the scattering in the AdS space, and involves various quantities. First, to describe the transition  $\gamma^*N \rightarrow \gamma^*N \equiv 1, 2 \rightarrow 3, 4$ , states dual to the initial-final nucleon  $N$  are required, i.e. the hadronic state  $|PQ\rangle$  in (3). These states are represented by normalizable wave functions  $\phi^N(z)$  depending on the holographic coordinate  $z$  (positive and with the UV brane corresponding to  $z = 0$ ), and are obtained in principle from a suitable equation of motion. The calculation of the matrix element (3) involves the transition function

$$P_{24}(z) = \sqrt{-g} \left( \frac{z}{R} \right)^2 \phi^N(z) \phi^N(z) . \quad (5)$$

The current that couples to the hadrons in (3) induces non-normalizable modes of the gauge fields. In the bulk, such fields  $\mathcal{A}$  satisfy Maxwell’s equations of motion; their solutions, in the Lorentz gauge and for  $R = 1$ , are given in terms of Bessel functions:  $\mathcal{A}_\mu(y, z) = n_\mu(Qz)K_1(Qz)e^{iq \cdot y}$  and  $\mathcal{A}_z(y, z) = i(q \cdot n)(Qz)K_0(Qz)e^{iq \cdot y}$ , with  $n_\mu$  a polarization vector. To determine the structure function  $F_2$  in (3) a transition function  $P_{13}$  is needed, and is given by [4, 5]

$$P_{13}(z, Q^2) = \frac{1}{z} (Qz)^2 [K_0^2(Qz) + K_1^2(Qz)] \quad (6)$$

with  $Q = \sqrt{Q^2}$ .

The last ingredient is the scattering kernel. This has been expressed in terms of a Pomeron Regge pole contribution [7], and allows to write the structure function  $F_2$  at low- $x$  as an eikonal sum with a convolution of the transition functions (5) and (6) [4]:

$$\begin{aligned} F_2^N(x, Q^2) &= \frac{Q^2}{2\pi^2} \int d^2b \int dz dz' P_{13}(z, Q^2) P_{24}(z') \\ &\quad \times \text{Re} \left( 1 - e^{i\chi(s, b, z, z')} \right) . \end{aligned} \quad (7)$$

$b$  is the impact parameter, with  $\vec{b}$  the transverse Minkowski space vector for  $\gamma^*p$  scattering;  $s$  is the center-of-mass energy squared of the  $\gamma^*$ -target system. The eikonal  $\chi$  can be derived for conformal theories; it can also be modified by the inclusion of conformal symmetry-violating effects.

### Conformal limit

For conformal fields the free nucleon structure function  $F_2^N$  can be obtained from (7) and is given by [4]

$$F_2^N(x, Q^2) = \frac{g_0^2 \rho^{3/2}}{32\pi^{5/2}} \int dz dz' \frac{z z' Q^2}{\tau^{1/2}} P_{13}(z, Q^2) P_{24}(z') \times e^{(1-\rho)\tau} \exp[\Phi(z, z', \tau)] , \quad (8)$$

where  $x \simeq Q^2/s$  and  $g_0^2$  a constant. The conformal invariant  $\tau$  is defined as  $\tau = \log(\rho z z' s/2)$ . The function  $\Phi$  is the BPTS Pomeron kernel integrated in impact parameter [7],

$$\Phi(z, z', \tau) = -\frac{(\log z - \log z')^2}{\rho\tau} . \quad (9)$$

The transition function  $P_{24}$  involves the nucleon wave function in the bulk  $\phi^N(z)$ . In ref.[4] it is assumed that the wave function  $\phi^N(z)$  is sharply peaked near the infrared boundary  $z_0$ , with  $1/Q' \leq z_0$  and  $Q'$  close to the nucleon mass:

$$P_{24}(z') \simeq \delta(z' - 1/Q') , \quad (10)$$

an expression adopted in the following. An explicit bulk model for the nucleon would be required to improve the wave function profile; modifications of this local approximation can be considered [17]. A further simplification consists in replacing also  $P_{13}$  by a local expression,

$$P_{13}(z, Q^2) \simeq C \delta(z - 1/Q) \quad (11)$$

with  $C \simeq 1$ . Since the integrand with  $P_{13}$  in Eq.(8) is peaked for  $z \simeq 1/Q$ , one can verify that this is a good approximation of Eq.(6). The resulting  $F_2$  reads [4]:

$$F_2^N(x, Q^2) = \frac{g_0^2 \rho^{3/2}}{32\pi^{5/2}} \frac{Q}{Q'} \frac{1}{\tau^{1/2}} e^{(1-\rho)\tau} e^{-[\log^2(Q/Q')/\rho\tau]} . \quad (12)$$

The nucleon structure function  $F_2^A$  at small  $x$  in a nuclear environment can be obtained rescaling the effective size of the nucleon wave function in the nucleus  $A$

$$Q'_A = \lambda_A Q' \quad (13)$$

in Eq.(12). In the conformal limit  $F_2$  depends on the ratio  $Q/Q'$  and therefore the rescaling  $Q'_A \rightarrow Q'$  corresponds to the  $Q^2$  rescaling  $Q^2 \rightarrow Q^2/\lambda_A^2$ . Hence, in this limit one has  $R_A = F_2^A/F_2^D$  neglecting the proton-neutron difference. Therefore, in the conformal limit the

$Q^2$ -rescaling at small  $x$  naturally arises in the AdS/CFT approach. This is not surprising, since the limit is reliable at large  $Q^2$ . Notice that in the local approximation (10,11),  $\tau = \log(\rho Q/2xQ')$ , therefore the rescaling  $Q'_A = \lambda_A Q'$  could be reabsorbed in  $x \rightarrow \lambda_A x$ . However, due to the  $Q^2$  dependence of  $F_2$  in Eq.(12), the  $x$ -rescaling is not completely equivalent to the rescaling in  $Q^2$ , and  $F_2^A(x, Q^2/\lambda^2) \neq F_2^A(\lambda x, Q^2)$ . The  $x$ -rescaling method in the holographic framework will be discussed in a dedicated study [17].

### Confinement effects

The expression for  $F_2^N$  for the free proton structure functions, based on the conformal BPST Pomeron, does not fit the HERA data in the low  $Q^2$  region, where confinement is the main dynamical mechanisms [4]. One needs to account for confinement, which can be described including an infrared boundary  $z_0$  on the  $z$  coordinate of the bulk. This scale could be related to the  $\Lambda_{QCD}$  parameter. It produces a mass gap, a modification of the eikonal and a non-conformal contribution to  $F_2^N$  which, for a single Pomeron, reads [4]:

$$F_{2ct}^N(x, Q^2, z_0) = \frac{g_0^2 \rho^{3/2}}{32\pi^{5/2}} \int dz dz' \frac{z z' Q^2}{\tau^{1/2}} P_{13}(z, Q^2) P_{24}(z') \times e^{(1-\rho)\tau} e^{-\frac{\log^2(z z' / z_0^2)}{\rho\tau}} G(z, z', \tau) . \quad (14)$$

In this expression the  $z_0$  dependence is shown explicitly;  $G(z, z', \tau)$  is given by

$$G(z, z', \tau) = 1 - 2\sqrt{\rho\pi\tau} e^{\eta^2} \operatorname{erfc}(\eta) , \quad (15)$$

and

$$\eta = \frac{-\log(z z' / z_0^2) + \rho\tau}{\sqrt{\rho\tau}} . \quad (16)$$

With the local approximation (10,11), Eq.(14) reduces to

$$F_2^N(x, Q^2, Q_0^2) = \frac{g_0^2 \rho^{3/2}}{32\pi^{5/2}} \frac{(Q/Q')}{\tau^{1/2}} e^{(1-\rho)\tau} \times e^{-\frac{\log^2(Q_0^2/(QQ'))}{\rho\tau}} G\left(\frac{1}{Q}, \frac{1}{Q'}, \tau\right) , \quad (17)$$

where  $Q_0 = 1/z_0$  [4].

In the description of nuclear effects by the rescaling  $Q'_A = \lambda_A Q'$ , the  $\tau$  dependence on the ratio  $Q/Q'$  is remarkable, and would suggest a  $Q^2$ -rescaling. However, there is also a nontrivial  $Q^2$  behavior in the log-factors and in  $\eta$  due to the new scale  $Q_0$ . The dependence on  $Q_0$  in Eq.(14) is in the form  $Q_0^2/QQ'$ ; therefore, the rescaling  $Q'_A = \lambda_A Q'$  can be reabsorbed in the  $Q^2$  rescaling  $Q^2 \rightarrow Q^2/\lambda_A^2$  provided that the confinement distance in nuclear environment scales in the same way,

$$Q_0^2 \rightarrow Q_0^2/\lambda_A^2 . \quad (18)$$

Our phenomenological analysis is done using this rescaling of  $Q_0$  at fixed  $x$ .

## COMPARISON WITH NUCLEAR DIS DATA, COMMENTS AND CONCLUSIONS

The knowledge of structure functions and parton distribution functions in nuclei is important in relativistic heavy ion collisions, since the “hard probes” of the quark-gluon plasma require a control of cold nuclear effects, i.e. the modifications depending on the nuclear dynamics [14, 18, 19].

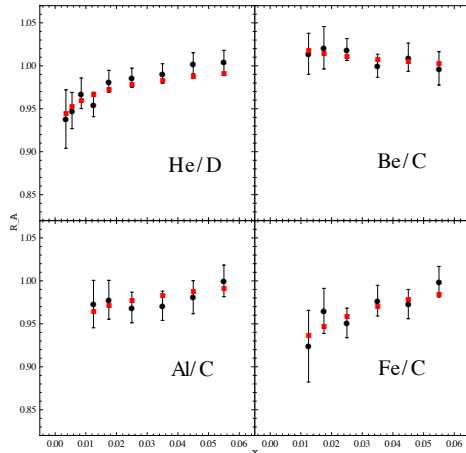


Figure 1: Experimental data (black points) [21] and AdS/CFT results based on  $Q^2$ -rescaling (red squares) for various nuclei. The values of the experimental average  $Q^2$  (in  $\text{GeV}^2$ ), from the first to the last bin in  $x$ , vary in the ranges [0.77 – 6.3] (He/D), [3.4 – 9.8] (Be/C), [3.4 – 11.6] (Al/C), [3.4 – 11.8] (Fe/C). The theoretical values are obtained by Eq.(19) using the experimental average  $Q^2$  for given  $x$  and the  $\lambda_A$  parameters in the first column of Table I. The  $\chi^2/d.o.f.$  is 1.09 (He/D), 0.21 (Be/C), 0.23 (Al/C) and 0.41 (Fe/C).

The results of the holographic approach can be compared to experimental data [21] by applying the  $Q^2$  rescaling scheme based on Eqs.(12,18): when  $Q'_A = \lambda_A Q'$  one rescales  $Q^2 \rightarrow Q^2/\lambda_A^2$  and  $Q_0^2 \rightarrow Q_0^2/\lambda_A^2$ . The  $Q^2$  rescaling is exact not only in the conformal part but also in the confinement contribution. This implies

$$F_2^A(x, Q^2) = F_{2,cl}^N \left( x, \frac{Q^2}{\lambda_A^2} \right) + F_{2,ct}^N \left( x, \frac{Q^2}{\lambda_A^2}, \frac{Q_0^2}{\lambda_A^2} \right), \quad (19)$$

with the conformal term  $F_{2,cl}^N$  in Eq.(12) and the confinement one  $F_{2,ct}^N$  in Eq.(17). For each nucleus there is only one parameter  $\lambda_A$ .

Fig.1 and 2 report the comparison of the theoretical results with NMC data [21] in the small- $x$  region,  $x \leq 0.07$ , for different nuclei. The theoretical values are obtained using the average  $Q^2$  for a given  $x$ , the other parameters being fixed as in [4]. The agreement with data is remarkable, despite the neglect of the proton and neutron structure function difference. The optimization of the parameters  $\lambda_A$  and a complete analysis is presented else-

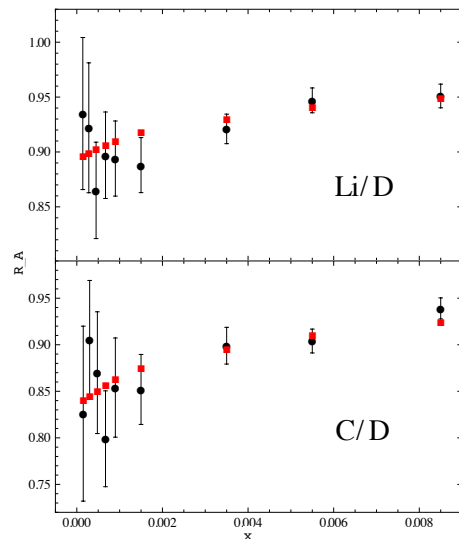


Figure 2: Low- $x$  experimental data for  $R_A$  (black points) [21] compared to holographic results (red squares) for different nuclei. The experimental average  $Q^2$  (in  $\text{GeV}^2$ ), from the first to the last bin in  $x$ , varies in the ranges [0.034 – 1.4] (Li/D), [0.035 – 1.6] (C/D). The theoretical values are obtained using Eq.(19) and the experimental average  $Q^2$  for given  $x$ . The  $\chi^2/d.o.f.$  is 0.93 (Li/D) and 1.61 (C/D).

where [17]; considering the neutron-proton isospin breaking improves the  $\chi^2/d.o.f.$

Understanding the agreement of the holographic result with nuclear data is easier if we consider the origin of (13) and (18). In the AdS/CFT framework, this comes from the identification of the bulk coordinate with the energy scale of the dual theory: considering the form of the  $AdS$  metric in Poincaré coordinates, a coordinate rescaling  $x_\mu \rightarrow \lambda x_\mu$  on the boundary corresponds to  $z \rightarrow \lambda z$  in the bulk. In nuclei, due to the nucleon overlap, the average distance among quarks and gluons decreases and the color neutralization infrared (confinement) scale increases. Such modifications in the boundary correspond in the bulk, respectively, to  $z' \rightarrow z'/\lambda$  and  $z_0 \rightarrow \lambda z_0$ , i.e. the prescription employed to describe the nuclear effects by the momenta redefinition. The dynamical generation of the effective IR scale remains to be clarified, with a possible analogy with the generation of the saturation scale in free nucleon within this framework [20].

The method inspired by AdS/CFT provides a description of the nuclear effects in the DIS structure functions based on  $Q^2$ -rescaling which corresponds to a geometrical scaling of the confinement size for a bound nucleon. The same result can be obtained in other, rather different, frameworks. Indeed, at high energy, the structure functions can be evaluated in the QCD dipole model [22, 23] where the virtual photon  $\gamma^*$  splits in a quark-antiquark dipole interacting with the target ( $T$ ). Assuming, within

this model, that the energy and target size dependence of the dipole-target cross section  $\sigma^{\gamma^*T}$  can be encoded in a saturation scale  $Q_{S,T}(x)$  [24], that there is no dependence of the dipole wave function on the quark and antiquarks distribution of the longitudinal momenta [25], and that there is a minor dependence of the saturation scale on the specific scattering process, the dimensionless ratio  $\sigma^{\gamma^*T}/\pi R_T^2$  depends only on  $\tau_T^2 = Q^2/Q_{S,T}^2(x)$ . The geometric scaling between the nucleus and the nucleon cross sections [24]

$$\frac{\sigma^{\gamma^*A}(\tau_A)}{\pi R_A^2} = \frac{\sigma^{\gamma^*N}(\tau_N)}{\pi R_N^2}, \quad (20)$$

with radii  $R_{N,A}$  and

$$\tau_A^2 = \tau_N^2 \left( \frac{\pi R_A^2}{A\pi R_N^2} \right)^{1/\delta}, \quad (21)$$

implies the relation

$$Q_{S,A}^2 = Q_{S,N}^2 \left( \frac{A\pi R_N^2}{\pi R_A^2} \right)^{1/\delta}. \quad (22)$$

The relation between the structure function per nucleon  $F_2^A$  and  $\sigma^{\gamma^*A}/\pi R_A^2$  involves the factor  $Q^2\pi R_A^2/A$ , which can be approximated by  $Q^2/Q_{S,A}^2$  if the  $x$ -dependence of the saturation scale is neglected. As a result, the dependence of  $F_2^A$  on  $Q^2/Q_{S,A}^2$  corresponds to rescaling  $Q^2 \rightarrow Q^2/\lambda_{A,dip}^2$ , with

$$\lambda_{A,dip} = \left( \frac{A\pi R_N^2}{\pi R_A^2} \right)^{1/2\delta}. \quad (23)$$

A good fit of low- $x$  nuclear data in the dipole model is obtained for  $R_A = (1.12A^{1/3} - 0.86A^{-1/3})$  fm,  $\pi R_N^2 = 1.55$  fm<sup>2</sup> and  $\delta = 0.79$  [24].

In Table I we compare the parameters  $\lambda_A$  obtained in the holographic framework and in QCD dipole picture. Although the theoretical approaches are different, the deviation in this parameter is restrained in the range 5% – 11% going from Li to Fe; for Pb the deviation is about 32%.

A	$\lambda_A(\text{AdS/CFT})$	$\lambda_{A,dip}$ [24]	$\lambda_{A,nuc}$ [11]
Li	1.069	1.125	1.045
Be	1.073	1.128	1.077
C	1.111	1.143	1.104
Al	1.184	1.243	1.140
Ca	1.219	1.315	1.137
Fe	1.251	1.387	1.154
Pb	1.327	1.755	1.188

Table I:  $\lambda_A$  obtained using  $F_2$  in the holographic approach, compared to the QCD dipole picture [24] and the change in the nucleus confinement size due to two-nucleon overlap [11].

The rescaling  $Q_0 \rightarrow Q_0/\lambda_A$  corresponds to the modification  $z_0^A = \lambda_A z_0$ , that is to an increase of the confinement size in nuclei. It is interesting to compare the results also with the changes in the confinement size in a nucleus  $\lambda_{A,nuc}$  evaluated by the overlap of two nucleons interacting by a Reid soft-core potential [11], reported in Table I. In this case the deviation on  $\lambda_A$  is between 4% and 8% from Li to Fe, and 12% for Pb.

The modification of the confinement sizes is a dynamical property of the bound nucleons, independent of  $x$ , which permits the description of nuclear effects at low- $x$ . On the other hand, at larger  $x$  one has the EMC and anti-shadowing regions. A general approach in the whole kinematical region  $0 < x < 1$  is still lacking, but a  $Q^2$  rescaling, although with different features for large and low- $x$ , could be the unifying dynamical element. We have found that, starting from a gauge-gravity duality approach, a reliable description of nuclear shadowing can be obtained rescaling the virtual photon scale  $Q^2$  “seen” by a parton in a bound nucleon.

- 
- [1] J. M. Maldacena, *Adv. Theor. Math. Phys.* **2**, 231 (1998) [*Int. J. Theor. Phys.* **38**, 1113 (1999)]; S. S. Gubser, I. R. Klebanov and A. M. Polyakov, *Phys. Lett. B* **428**, 105 (1998); E. Witten, *Adv. Theor. Math. Phys.* **2**, 253 (1998).
- [2] See, e.g., J. Erlich, E. Katz, D. T. Son and M. A. Stephanov, *Phys. Rev. Lett.* **95**, 261602 (2005); O. Aharony, J. Sonnenschein and S. Yankielowicz, *Annals Phys.* **322**, 1420 (2007); J. Casalderrey-Solana, H. Liu, D. Mateos, K. Rajagopal and U. A. Wiedemann, arXiv:1101.0618 [hep-th].
- [3] J. Polchinski and M. J. Strassler, *Phys. Rev. Lett.* **88**, 031601 (2002); *JHEP* **0305**, 012 (2003).
- [4] R. C. Brower, M. Djuric, I. Sarcevic and C. -I Tan, *JHEP* **1011**, 051 (2010).
- [5] B. Pire, C. Roiesnel, L. Szymanowski and S. Wallon, *Phys. Lett. B* **670**, 84 (2008).
- [6] M. Arneodo, *Phys. Rept.* **240**, 301 (1994).
- [7] R. C. Brower, J. Polchinski, M. J. Strassler and C. -I Tan, *JHEP* **0712**, 005 (2007).
- [8] B. Povh and J. Hufner, *Phys. Rev. Lett.* **58**, 1612 (1987).
- [9] S. V. Akulinichev et al., *Phys. Lett. B* **158**, 485 (1985); *Phys. Rev. Lett.* **55**, 2239 (1985).
- [10] F. E. Close, R. G. Roberts and G. G. Ross, *Phys. Lett. B* **129**, 346 (1983); R. L. Jaffe, F. E. Close, R. G. Roberts and G. G. Ross, *Phys. Lett. B* **134**, 449 (1984); R. L. Jaffe, *Phys. Rev. Lett.* **50**, 228 (1983).
- [11] F. E. Close, R. L. Jaffe, R. G. Roberts and G. G. Ross, *Phys. Rev. D* **31**, 1004 (1985).
- [12] F. E. Close, R. G. Roberts and G. G. Ross, *Phys. Lett. B* **168**, 400 (1986); R. P. Bickerstaff and G. A. Miller, *Phys. Lett. B* **168**, 409 (1986).
- [13] A. H. Mueller and J. -w. Qiu, *Nucl. Phys. B* **268**, 427 (1986); J. -w. Qiu, *Nucl. Phys. B* **291**, 746 (1987).
- [14] K. J. Eskola, H. Paukkunen and C. A. Salgado, *JHEP* **0904**, 065 (2009).
- [15] P. Castorina and A. Donnachie, *Phys. Lett. B* **215**, 589

- (1988); Z. Phys. C **45**, 141 (1989).
- [16] For other ways of breaking the conformal invariance see: S. S. Gubser, hep-th/9902155; U. Gursoy and E. Kiritsis, JHEP **0802**, 032 (2008); U. Gursoy, E. Kiritsis and F. Nitti, JHEP **0802**, 019 (2008).
- [17] L. Agozzino, P. Castorina and P. Colangelo, arXiv:1401.0826.
- [18] K. J. Eskola, V. J. Kolhinen, H. Paukkunen and C. A. Salgado, JHEP **0705**, 002 (2007).
- [19] A. Accardi, F. Arleo, N. Armesto, R. Baier, D. G. d'Enterria, R. J. Fries, O. Kodolova, I. P. Lokhtin *et al.*, hep-ph/0310274.
- [20] L. Cornalba and M. S. Costa, Phys. Rev. D **78**, 096010 (2008); Y. Hatta, E. Iancu and A. H. Mueller, JHEP **0801**, 026 (2008).
- [21] P. Amaudruz *et al.* [New Muon Collaboration], Nucl. Phys. B **441**, 3 (1995); M. Arneodo *et al.* [New Muon Collaboration], Nucl. Phys. B **441**, 12 (1995); M. Arneodo *et al.* [New Muon Collaboration], Nucl. Phys. B **481**, 3 (1996).
- [22] N. N. Nikolaev and B. G. Zakharov, Z. Phys. C **49**, 607 (1991).
- [23] A. H. Mueller, Nucl. Phys. B **415**, 373 (1994).
- [24] J. L. Albacete, N. Armesto, J. G. Milhano, C. A. Salgado and U. A. Wiedemann, Eur. Phys. J. C **43**, 353 (2005); J. L. Albacete, N. Armesto, J. G. Milhano, C. A. Salgado and U. A. Wiedemann, Phys. Rev. D **71**, 014003 (2005).
- [25] D. Schildknecht, Phys. Lett. B **716**, 413 (2012).